NOTES AND CORRESPONDENCE

On the Clearing of Cumulus Clouds Downwind from Lakes

M. SEGAL, R. W. ARRITT, J. SHEN, C. ANDERSON, AND M. LEUTHOLD

Department of Agronomy, Iowa State University, Ames, Iowa

26 March 1996 and 30 July 1996

ABSTRACT

In this note the forcing of cumulus cloud clearing over and downwind from lakes during the warm season is evaluated conceptually by modeling and observational approaches. It is suggested that drying by dynamically induced subsidence and suppression of the CBL over the lake mutually contribute to the cloud clearing. The effect of background flow speed and the extent of potential clearing area is illustrated. Various implications of the cloud clearing are discussed.

1. Introduction

Clearing of fair weather and shallow cumulus clouds in the downwind direction (in the sense of the background wind) from lakes is an observed feature in various geographical locations during the warm season. Similar clearing often is observed over bays or wide rivers. Some lakes are located in valley basins where cumulus cloud clearing may be supported by the compensating subsidence resulting from daytime thermally induced upslope circulations, or by dynamically induced subsidence associated with background flow crossing the elevated topography. However, the clearing of cumulus clouds is typical also for lakes located in flat terrain. Purdom (1990), Rabin et al. (1990), Gibson and Vonder Haar (1990), for example, present satellite illustrations of such clearing. The area affected by cloud clearing may be of the same size as the lake characteristic width or even much larger. Although these cloud clearing features are easily recognized from visible satellite imagery and are considered by local forecasting offices, there has not been a focused and direct evaluation of the physical processes that produce the clearing. In numerical model simulations of south Florida, Pielke (1974) shows that the flow divergence field downwind from Lake Okeechobee acquires a ''plume'' shape in which the lake breeze (LB) can be identified. The lateral boundaries of the plume consist of convergence caused by the contrast between the LB and the background flow. Numerical model simulations studying the interaction of lake breezes (LB) and background flows (e.g., Physick 1976; Gross and Estoque 1981; Segal and Pielke 1985; Arritt 1989) have indirectly examined various characteristics pertinent to the cloud clearing but have not addressed this situation in detail. In this note, preliminary general evaluations of the forcing of the cloud clearing for flat terrain situations are provided including conceptual elaborations, numerical model results, and observations.

2. Conceptual and modeling evaluations

The combination of three main physical forcings are suggested to be the cause of the cloud clearing over the lakes and land areas in the downwind direction. These include (i) subsidence induced by the coupling of LB and background flow, (ii) modification of the convective boundary layer (CBL) depth and thermodynamic properties, and (iii) modification of the lower atmosphere flow due to changes in turbulence.

Conceptual evaluations of the contribution of each process are outlined in the following subsections. In support of these evaluations, illustrative 2D numerical model simulations were carried out for a lake of 32-km width when background flows of 2 and 8 m s^{-1} were prescribed. The numerical model is a version of the model described by Arritt (1989) with extension to nonhydrostatic quasi-compressible governing equations as described by Siems and Bretherton (1992). The model horizontal and vertical grid resolution were 1000 and 50 m, respectively. The input soil parameters in the simulations reflect July conditions around Lake Okeechobee, Florida. Likewise, the meteorological initial conditions corresponded to those that prevailed at the early morning on 9 July 1995 in the vicinity of Lake Okeechobee during the Lake Breeze Experiment (LABEX) field project (Arritt et al. 1996). The noon Bowen

Corresponding author address: Moti Segal, Department of Agronomy, Iowa State University, 3010 Agronomy Hall, Ames, IA 50011.

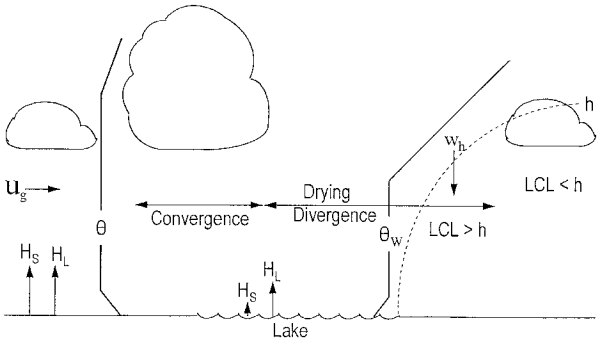

FIG. 1. A schematic illustration of features associated with cumulus cloud clearing downwind from a lake (see text for an explanation of the notation).

ratio (predicted over the land) was approximately 1. The evaluations presented here consider also the relationship between the background flow intensity and the area affected by clearing of clouds.

a. Subsidence induced by the coupling of lake breeze and the background flow

Flow convergence is generated due to the coupling of the LB with the background flow in the windward shore of the lake, whereas flow divergence is generated over the lake and extends onto the land in the downwind direction. Figure 1 provides a schematic illustration of features related to this situation (and additional aspects evaluated in this note).

In the absence of background flow during the day, subsidence induced by the LB develops over the lake, and it extends gradually onshore with the movement of the LB front. When the extended surroundings of the lake are affected by cumulus clouds, these subsidence areas, as in the case of sea breezes, are apparent as clear regions. When background flow exists, the dynamical coupling of the background flow and the LB results in an area of subsidence, which is extended and shifted in the downwind direction. The subsidence has three roles in contributing to clearing: (i) descending air above the CBL where upward motion by thermal eddies is not experienced; (ii) thermal stabilization of the lower atmosphere and enhancement of capping inversion structures; (iii) as is typical above the CBL, the specific humidity drops, so that the downward advection through the CBL top reduces the specific humidity within the CBL, and the lifting condensation level (LCL) increases. These subsidence related processes are conducive to dissipation of cumulus clouds over the lake and for some distance downwind from the leeward shore. For weak background flow compared with the LB speed, the induced subsidence pattern is somewhat distorted as compared with the calm background situation. Based on previous results for simulated sea breezes, the strongest subsidence is likely when the background flow and the LB are about of comparable intensity (Arritt 1993). When the background flow is strong enough to dominate the induced LB, both the convergence and subsidence intensity reduce. The clearing area may be of reduced extent or altogether absent if the subsidence is too weak to counteract vigorous CBL thermals.

Figures 2a and 2b, respectively, illustrate the simulated coupling of LB with background flows of $u_g = 2$ m s^{-1} and 8 m s^{-1}. The well-known features of suppression of windward shore LB flow and intensification of the flow above the LB layer are simulated (Figs. 2a,b). For the case of $u_g = 2$ m s^{-1}, the LB circulation cells are revealed near both shores. However, for $u_g = 8$ m s^{-1} the windward shore LB circulation cell is very shallow and weak, and the lee shore LB cell is diminished compared with the $u_g = 2$ m s^{-1} case. Figures 2c,d provide the corresponding simulated vertical velocity cross sections. The convergence zone generated by the coupling of the background flow and the LB is followed by an extensive subsidence area covering the lake and extending downwind.

The flow pattern resembles that of synoptic flow crossing an ''apparent ridge'' (the ''apparent ridge'' is represented by the dashed contours cross section in Figs. 2a,b; the contour $u = 0$ delineates the ''apparent ridge'' surface). The ''apparent ridge'' consists of a local perturbation in the synoptic flow that is produced by the differential surface heating and corresponds approximately to the LB layer. Unlike a real ridge where atmospheric mass is constrained by the terrain surface, in an ''apparent ridge'' the exchange of air mass between the ''ridge'' and the flow above it is possible through the induced vertical motion or turbulence. Similar to a topographic ridge, convergence is generated on the windward side of the ''apparent ridge'' (however, the convergence associated with the LB circulation cell for light background flows would be stronger than that of an ''apparent'' ridge) followed by subsidence on its leeward side, which covers most of the lake and some inland section on the lee shore. However, with an ''apparent ridge'' the flow features are distorted, and impact on flow is weaker compared with a true ridge situation. For the $u_g = 2$ m s^{-1} simulation, the ''apparent ridge'' height is about double that corresponding to the $u_g = 8$ m s^{-1} simulation, whereas the corresponding characteristic width is almost unchanged. Consequently, the relative intensification of horizontal flow above the ''apparent ridge'' top is larger in the first case (although the absolute magnitude of the increase in the flow is similar in both cases). The peak upward velocities at the convergence zones are similar for both cases, however, the subsidence velocities are larger in absolute magnitude for the $u_g = 2$ m s^{-1} case (Figs. 2c,d).

From a scaling point of view, we may assume that the average intensity of the subsidence is related to that of the vertical velocity in the convergence zone w_u. Conceptually, w_u is constrained by

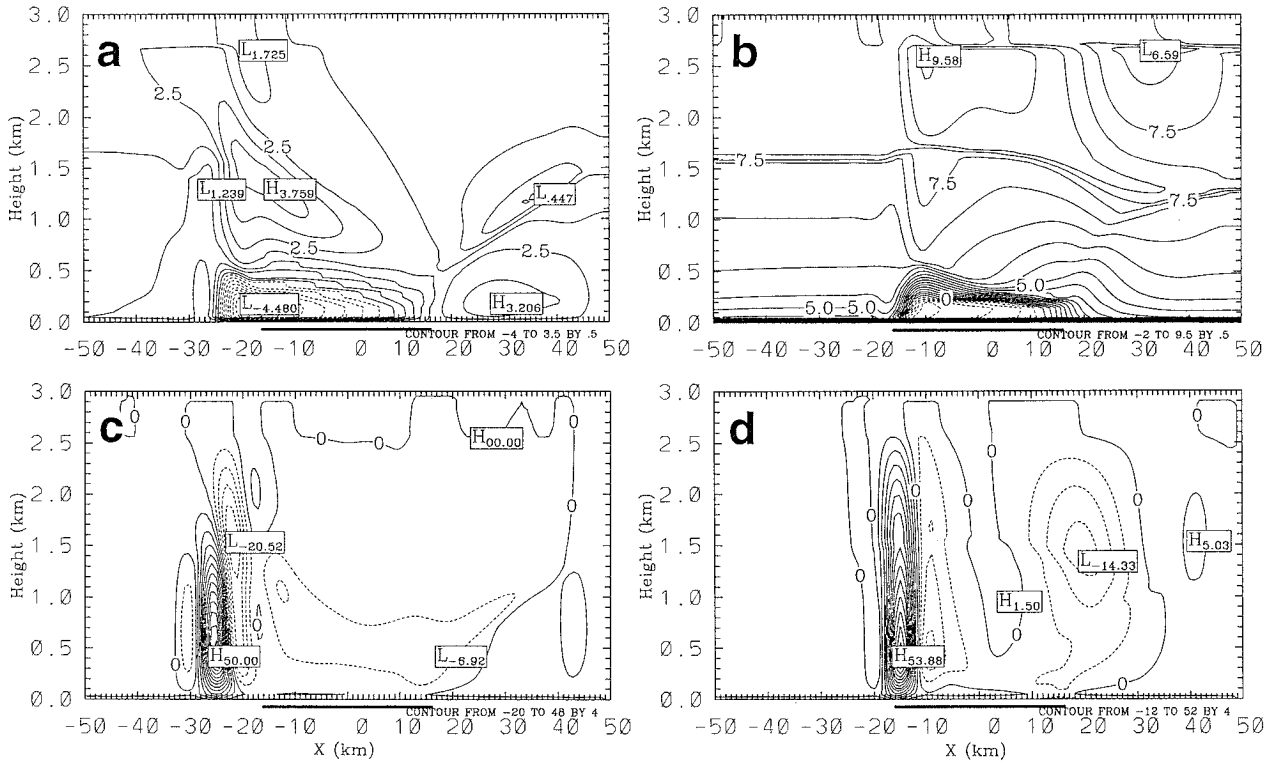

FIG. 2. Vertical cross section of simulated 32-km width elongated lake at 1400 LST with corresponding background flow $u_g = 2$ m s^{-1} and $u_g = 8$ m s^{-1}. (a) and (b) Simulated cross-lake flow (m s^{-1}), contour interval 0.5 m s^{-1}; (c) and (d) vertical velocities (cm s^{-1}) contour interval of 4 cm s^{-1}. The lake location is indicated by the dark line. Here, ''H'' and ''L'' indicate local maximum and minimum values.

$$w_u = \max\left[w_{\mathrm{LB}}, u_g \frac{\partial Z(u = 0)}{\partial x}\right], \tag{1}$$

where $Z(u = 0)$ is the altitude of the surface for which $u = 0$. The first term in the parenthesis is the upward vertical velocity generated because of convergence directly associated with the lake breeze direct flow. The second term is upward motion generated by the ''apparent ridge'' effect. For light u_g the first term dominates, whereas for higher values of u_g the second one dominates (see Figs. 2a–d; for $u_g = 2$ m s^{-1} the location of the peak vertical velocity is directly associated with LB, i.e., with the horizontal gradient in the onshore flow, whereas for $u_g = 8$ m s^{-1} the peak upward vertical velocity is directly associated with the ''apparent ridge'' slope, i.e., with the horizontal gradient in the background flow). However, above some threshold u_g the value of the second term should reduce with increase in u_g, because of a corresponding faster decrease of $\partial Z(u = 0)/\partial x$. This is most likely to occur in the regime where u_g is strong enough to overwhelm the dynamical response to differential heating (Arritt 1993).

b. Modification of CBL depth and thermodynamic properties

1) THE CBL DEPTH AND TKE FIELD

For advection of a relatively warm air mass over a relatively cool lake, the surface moist enthalpy flux (i.e., the sum of the surface sensible, H_s, and the latent heat flux, H_L) from the lake to the atmosphere is small compared with that over the land. [For moderate wind speed and water–air temperature difference, the moist enthalpy flux over the lake is typically one order of magnitude lower than that over the land (e.g., Garratt 1994).] Thus, as the air passes over the lake, the development of the CBL stops. As the remnant CBL traverses the lake, it is modified by the following processes: (i) significant reduction of buoyant turbulence production because of the reduction in surface sensible heat flux H_s into the atmosphere, or its cessation when the advected air is warmer than the surface water and a stable surface layer is onset; (ii) viscous dissipation of turbulence generated earlier over the land; (iii) induced subsidence by flow divergence, which reduces the CBL depth, while enhancing its capping temperature inversion; (iv) radiative cooling of the air (which intensifies with the decrease of the lake surface temperature).

Adopting a Lagrangian approach for an atmospheric column advected over the lake, we can scale the redevelopment of the CBL downwind from the windward shore (see Fig. 1 for a schematic illustration). We assume that over the land the CBL is about neutrally stratified, whereas over the lake the thermal stabilization results in an average vertical gradient of potential temperature $\beta_w = \partial\theta_w/\partial z > 0$ (the subscript w indicates an overwater

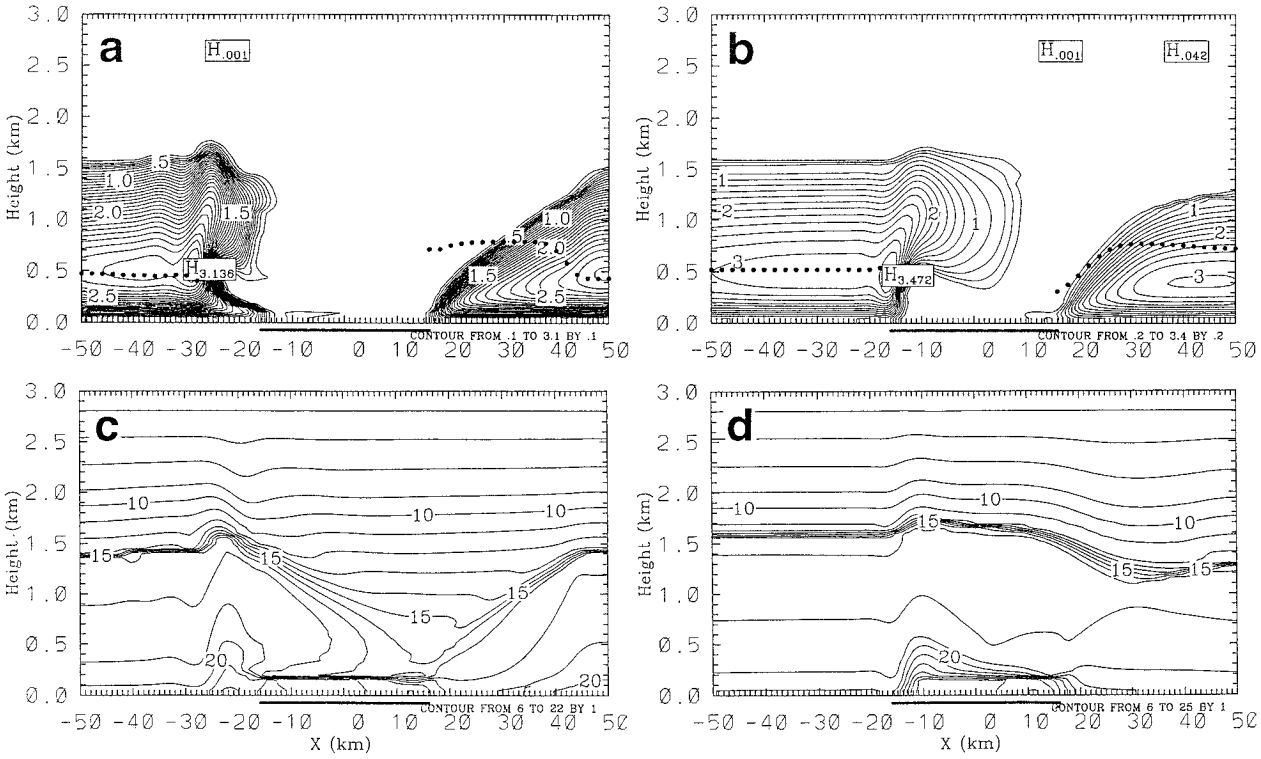

FIG. 3. The same as Fig. 2 except for (a) and (b) TKE ($m^2\ s^{-2}$); dots indicate the LCL height (m), (c) and (d) the specific humidity ($g\ kg^{-1}$).

location) by the time that the column has traversed the lake. Upon reaching the lee shore, H_s increases and gradual deepening of the CBL is initiated, with its depth h_{tL} at onshore distance L approximated as

$$h_{t_L} = \left(\frac{2C_\theta \int_0^{t_L} H_s\, dt}{\rho_a C_p \beta_w} \right)^{1/2} + w_h t_L, \qquad (2)$$

where $C_\theta (\simeq 1.2)$ is the CBL top entrainment coefficient; ρ_a and C_p are the air density and specific heat at constant pressure, respectively; $t_L = L/u$ (where u is the averaged speed of the onshore flow); and w_h is the typical subsidence vertical velocity at the CBL top. Equation (2) can be approximated as (substituting typical numerical values of ρ_a and C_p in SI units):

$$h_{t_L} = 4.5 \times 10^{-2} \left(\frac{\overline{H}_s t_L}{\beta_w} \right)^{1/2} + w_h t_L, \qquad (3)$$

where $\overline{H}_s$ is the averaged H_s (over land) during time t_L. Using (3), the relative importance of the sensible heat flux, the thermal stratification over the water and the subsidence can be scaled. For example, for $t_L = 1000$ s, $\overline{H}_s = 250$ W m^{-2}, $\beta_w = 2.5 \times 10^{-3}$ K m^{-1}, and $w_h = -0.1$ m s^{-1} the first term on the rhs of (3) would result in growth of about 450 m of the CBL due to sensible heat flux, whereas the subsidence would result in suppression of about 100 m. In general, the relative importance of the various environmental parameters in the recovery of the CBL is implied by the relation (3). The value of $\overline{H}_s$ is affected by land use and may be as high as approximately 400 W m^{-2} for a dry surface. The value of β_w is dependent on w_h, lake size, and lake surface water temperature, while w_h is dependent on the speed of the background flow, lake size, and the land use surrounding the lake.

Figures 3a,b illustrate the simulated TKE (turbulent kinetic energy) field for cases with $u_g = 2$ m s^{-1} and $u_g = 8$ m s^{-1}. An immediate drop in the TKE was simulated at the edge of the convergence zone, while the TKE is suppressed over the entire lake area for the weaker background flow. For the stronger flow, TKE is advected somewhat offshore. The turbulence decays from the surface upward in a manner that is analogous to the decay of CBL turbulence after abrupt cessation of the surface sensible heat flux (Nieuwstadt and Brost 1986). On the lee shore the build-up of a CBL, as evident by the TKE spatial distribution downwind from the lake, indicates a gradual deepening of the CBL with increasing onshore distance.

2) THE SPECIFIC HUMIDITY

Figures 3c,d present the simulated vertical cross section of the specific humidity. The high specific humidity

prescribed in the initial profile as well as the relatively wet land surface contributed to high values of simulated specific humidity by 1400 LST. It is worth noting that the available LABEX radiosonde observations support this feature of high specific humidity until late in the morning. It appears, however, that later change due to large-scale advection (which is not accounted for in the model simulations) resulted in lower values of observed specific humidity during the afternoon. Over the lake, contribution from the water surface evaporation was confined in a shallow layer because turbulent mixing was weak (the corresponding q values appear to be somewhat excessive). Downwind from the lake a pronounced drying is simulated in the $u_g = 2$ m s^{-1} case, compared with a milder drying for the $u_g = 8$ m s^{-1} simulation. The drying is the result of downward advection of relatively less humid air by the subsidence. The larger drying in the first case is attributed to weaker average horizontal advection, and greater horizontal width of the subsidence cell.

3) THE LCL HEIGHT

Initiation of cumulus clouds occurs some distance downwind from the lee shore once the CBL is deep enough. To produce fair weather cumulus cloudiness the constraint LCL $\leq h$ should be fulfilled, where h is the CBL depth and LCL is the lifting condensation level. Following Iribarne and Godson (1981) the LCL (in meters) can be approximated as

$$\text{LCL} \cong 4.2 \times 10^3 \, (-\log_{10}\text{RH}), \tag{4}$$

where RH is the lower atmosphere relative humidity (RH in the range 0–1).

The collapse of the CBL over the lake, which is accompanied by drying subsidence, results in effectively LCL $\gg h$ and a corresponding cloud clearing. Assuming for illustration that the potential temperature and specific humidity are conserved while moving downwind from the lake, then the cumulus clouds would reappear once the CBL depth reached the LCL in the upwind shore locations. In the real world, surface sensible heat flux would result in an increase in the potential temperature, whereas drying by the advective subsidence $w_h \, \partial q/\partial Z|_h$ at the top of the CBL reduces the specific humidity within the CBL. Thus, a decrease in RH and an increase in the LCL result. With the increase in $|w_h|$, the increase in horizontal extent of the subsidence cell, and the decrease of the specific humidity above the CBL top, the drop in the CBL specific humidity increases and correspondingly the area affected by clearing increases.

For scaling purposes, the relative significance of the subsidence drying effect is evaluated in the following. A step function change Δq_h at the top of the CBL is assumed. The ratio η of specific humidity sink due to subsidence to that of surface evapotranspiration source, $H_{L,}$ is considered as

$$\eta = \frac{\lambda \rho_{ah} w_h \Delta q_h}{H_L}, \tag{5}$$

where $\lambda (\cong 2500$ J g$^{-1})$ is the latent heat of evaporation. We assume representative values of $w_h = -0.1$ m s^{-1}, $\Delta q_h = 3$ g kg^{-1}, $\rho_{ah} = 1$ kg m^{-3}, and $H_L < 100$ W m^{-2} over the lake with $H_L < 600$ W m^{-2} over the land. Then, over the lake $\eta > 7$ and over the land $\eta \geq 1.2$, which indicate significant potential contribution of subsidence to cloud clearing over the lake and somewhat downwind from the lake.

The LCL for the simulations (Figs. 3a,b) were computed based on the averaged RH in the lower 1000 m. Upwind from the lake RH $\cong 0.75$ and the LCL $\cong 0.5$ km. Due to the drying, at some downwind distance clearly LCL $> h$, most noticeable for the $u_g = 2$ m s^{-1} case. Also typically the LCL in the area downwind from the lake is higher than in the upwind locations. However, the area affected by clearing is small compared with the lake width. Assuming RH $= 0.6$ in the upwind locations, which would be associated with an initially less humid lower atmosphere, then LCL $\cong 0.9$ km. The corresponding LCL height in the downwind direction would be even higher, resulting in further extension of the cloud-free area.

c. Modification of the lower-atmosphere flow

The downwind variation of the CBL described in section 2b forces restratification of the flow as a result of the related modifications in the turbulence fields. The reduction of turbulence over the lake should result in relative intensification of the flow, especially for heights great enough to be isolated from surface friction. The resulting horizontal gradients in the flow should contribute to induced subsidence over the lake. Generation of turbulence on the lee side of the lake contributes to flow reduction and to upward motion, though not dominating the subsidence generated motions. These effects are embedded in the simulated flow pattern presented in Figs. 2a,b and in the vertical velocity pattern Figs. 2c,d.

A simplified scaling is used to infer an upper limit for the characteristic vertical velocity W due to the differential friction. For this purpose it is assumed that a geostrophic flow with speed u_g crosses a 2D lake with width L. For illustrative purposes, we assume also that no LB is developed. Focus is made on a characteristic layer with depth H, which is the windward shore depth of the boundary layer. The characteristic speed increase across the lake within this layer due to cessation of turbulence is Δu. Then, from the continuity equation

$$W = -\frac{\Delta u}{L} H. \tag{6}$$

However, over the lake the flow is accelerated while undergoing inertial oscillations. Using the formulation

given in Garratt (1994, 176) the following scaling relation is applicable for narrow lakes:

$$\Delta u \leq \Delta \bar{u} f \frac{L}{u}, \tag{7}$$

where $\Delta\bar{u}(= u_g - u)$ is the characteristic difference between the geostrophic and observed wind u within the depth of the boundary layer in the windward shore, and f is the Coriolis parameter. Substituting (7) in (6) results in

$$|W| \leq \frac{\Delta \bar{u}}{u} fH. \tag{8}$$

Using characteristic values of $\Delta\bar{u}/u \leq 0.3$, $f = 10^{-4}$, $H = 1000$ m, yields: $|W| \leq 3$ cm s^{-1}. This magnitude of this induced subsidence is smaller by several factors compared to that obtained in the presented model simulations (see Figs. 2c,d).

3. Observations

During the LABEX project, radiosonde observations were taken near the shoreline of Lake Okeechobee at Clewston (C), the city of Okeechobee (O), and Pahokee (P) (see Fig. 4a for locations of the sites). Observations are presented for two days (9 July and 13 July 1995) on which the corresponding daytime lower atmosphere background flows were, respectively, westerly to northwesterly (2–5 m s^{-1}) and easterly to southeasterly (~6 m s^{-1}). No direct LB flow was observed at the onshore locations. GOES satellite visible imagery taken for southern Florida in these two days is used to provide observational insight into the cloud clearing patterns around Lake Okeechobee (Fig. 4). The images indicate clearing over the lake and through extended areas downwind from the leeward shore (east of the lake in the first case and northwest of the lake in the second case). The clear area at the presented hours is somewhat larger than the lake area. [Worth noting is that cumulus cloud clearings were sometimes evident over and downwind from wet areas (swamps): see, e.g., the clear area over the Everglades in the lower center of Fig. 4a. Clearing also was evident over and downwind of small lakes.]

Figure 5 presents the related skew T diagrams from NCAR CLASS soundings for these two days. Typically in the upwind shore formation of cumulus cloudiness is indicated by the air reaching near saturation within the CBL. In contrast, drying was observed over the downwind coasts, most noticeably in the altitude in which saturation was reached (LCL) in the upwind site. On 9 July at 1600 UTC (EST = UTC − 5 h), the LCL reached near the CBL top at C and O, whereas subsidence generated significant drying at P (Fig. 5a). The stabilization of the lower atmosphere at P due to subsidence is evident. Suppression of H_s over the lake resulted in noticeably cooler temperature in a near-surface layer of about 300-m depth at P. In the early afternoon

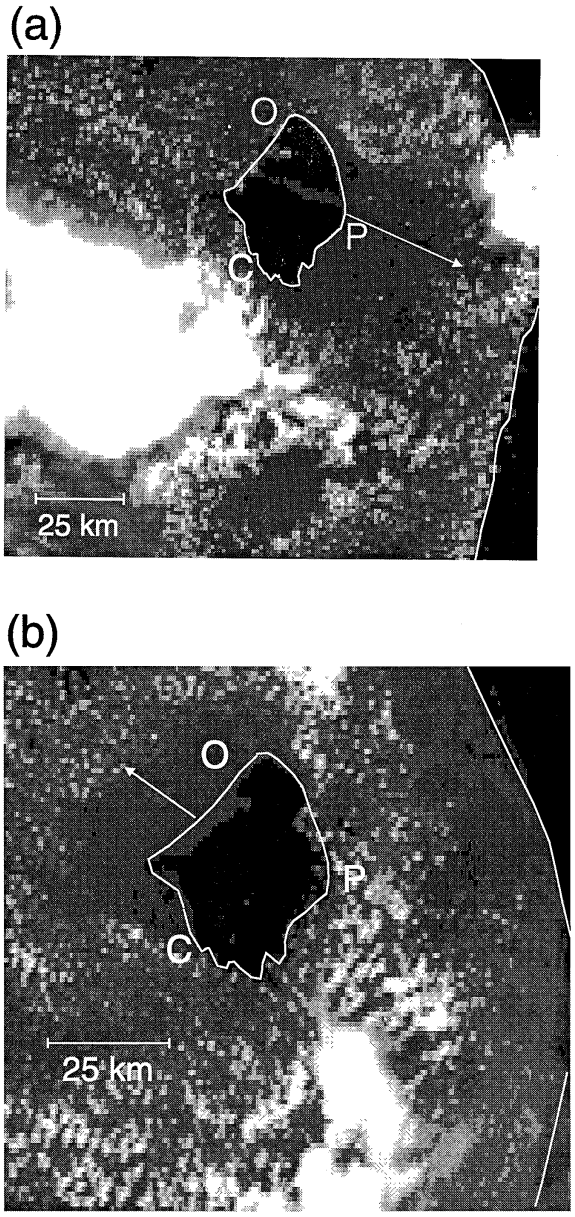

FIG. 4. GOES satellite visible images illustrating downwind clearing in Lake Okeechobee, Florida (indicated by the arrows): (a) 1700 UTC 9 July and (b) 1800 UTC 13 July (pixel resolution 1 km).

(1900 UTC; Fig. 5b), the southwestern portion of the lake was affected by deep convection as evident from the near-surface cooling at C. The earlier features of drying associated with stabilization at P persisted, whereas at C and O the CBL deepened and the LCL was lower than the CBL top. On 13 July (Figs. 5c,d) the flow direction differed by approximately 180° from that of the previous case resulting in a corresponding reversal of the features presented in Figs. 5a,b. At P the capping inversion was higher than at the windward shore locations C and O, whereas at C and O, lower-level thermal stabilization was evident at 1600 UTC and

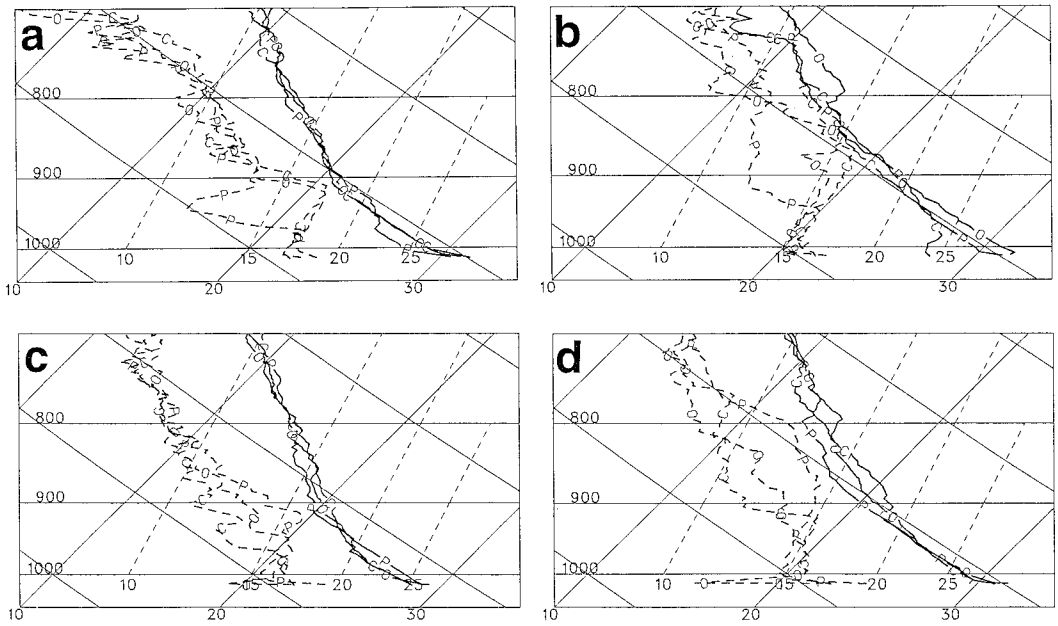

FIG. 5. Skew *T* illustrations for two cloud clearing days across Lake Okeechobee. The presented sites are Clewiston, the city of Okeechobee, and Pahokee (indicated by C, O, and P in Fig. 4): (a) 1600 UTC 9 July 1995, (b) 1900 UTC 9 July 1995, (c) 1600 UTC 13 July 1995, and (d) 1900 UTC 13 July 1995.

1900 UTC. The LCL was approached in P within the CBL. In contrast, drying was observed at C and O, and a cooler lower atmosphere was evident (1600 UTC and 1900 UTC) at C and O due to onshore flow.

4. Implications

a. Applied aspects

The extent and the width of the clearing area have implications in forecasting of summertime deep convection in the surroundings of lakes. Deep convection is unlikely to be initiated in these locations; however, it may spread into the clearing location through growth or movement of deep convection systems into this area. It was indicated for Lake Okeechobee based on observations that often there is enhancement in the cumulus field and deep convection initiated at the lateral edges of the clearing area (anonymous reviewer of this paper; G. Shaughnessy 1996, personal communication). In these locations, convergence resulting from the coupling of the LB and the background flow is likely. Therefore, it is probable that the location of the lateral edges of the clearing are quite important for thunderstorm forecasting. The clearing may also have significance in the implication of cloud shading effects in agricultural considerations, mostly when the background flow is persistent during the summer (e.g., Lake Okeechobee during midsummer, when easterly background flow is frequent). In the clearing area, increase of the daily evapotranspiration is likely. Photosynthesis may also increase, especially for crop species that do not become light-saturated (e.g., C_4 species such as maize, or sugar cane as in the Lake Okeechobee region).

b. Analogy with irrigated areas

Comparisons can be drawn between a lake and a similar-sized irrigated area, which may provide some insight into the influences such areas have on rainfall distribution. A subsidence zone should be produced over the irrigated area (when the irrigated area is surrounded by dry surface areas) as a result of coupling of background flow and thermally induced circulation (see section 2a). However, even for an irrigated area of exactly comparable size, subsidence may be weaker since sensible heat flux typically would be higher compared with that over cool water surfaces. The induced thermal circulations consequently should be weaker; and, therefore, the suppression of the CBL over the irrigated area as well as the drying due to subsidence would be less pronounced. Hence, the processes described in sections 2a and 2b would result in cumulus cloud clearing in the irrigated area, though likely less pronounced compared with the lake case. It has to be considered also, that unlike water surfaces, the surface enthalpy flux over the irrigated area in first approximation is the same as over the nonirrigated area. This should be conducive for faster downwind redevelopment of cumulus clouds. Satellite imagery over Florida indicates cloud clearing associated with the extremely wet locations such as swamps and impoundments. This is consistent with patterns reported in Curtim et al. (1995).

c. The reversed situation to cumulus clearing—Lake-effect snow

Lake-effect snow, physically, is a nearly reversed situation to the lake clearing evaluated in the present study. The previously described cloud-free area is converted into cloudy areas (typically manifested as stratiform clouds with embedded convective elements) when lake-effect snow is considered. It is worth outlining the differences in physical processes for these two cases, as it would provide a mutual complementary physical insight. Conceptual comparisons are made with the characteristics described in sections 2a and 2b. It is worth noting, however, that lake-effect snow tends to be enhanced when relatively large lakes (i.e., large fetch distance over the lake) are involved, when compared with much smaller lakes generating noticeable cloud clearing during the summer.

Comparing with sections 2a and 2b, for lake-effect snow situations, horizontal thermal conditions forcing a land breeze are likely to be involved (Passareli and Braham 1981). Coupling of the land breeze and the supportive background flow result in dynamic flow convergence over the lake. Also a reversed situation is generated while comparing with the process described in 2b. The advection of very cold air over the relatively warmer lake water results in an enhanced surface moist enthalpy flux and consequently to the generation and deepening of CBL, which is associated with moistening. This process is known to be the most important contribution enhancing cloud formation over the lake and downwind from the lee shore.

5. Conclusions

Preliminary general evaluations of cloud clearing over lakes and downwind from their lee shores were carried out by means of modeling, scaling, and observations. The evaluation indicated that the two most important processes contributing to the cloud clearing are: (i) The drying associated with subsidence that results from the lake breeze and its coupling with the opposing background flow. Therefore, the stratification of the background moisture should play a significant role in determination of the related impact. Drier air above the CBL top would result in stronger subsidence drying within the layer of the original CBL and thus contribute to enhanced cloud clearing. (ii) The gradual development of the CBL in the downwind area from the windward shore, which results in an LCL that is above the CBL top height for extended area.

Acknowledgments. The study was supported by NSF Grant ATM-9319455. This is journal paper J-16990 of Iowa Agricultural and Home Economics Experiment Station, Ames, Iowa, Project 3245, and supported by Hatch Act and State of Iowa funds. Observational support was provided by the NCAR Surface and Sounding Systems Facility and the University of Wyoming King Air during the LABEX project. Useful comments were provided by Geoffrey Shaughnessy and Eric Swartz and by the reviewers of this note. Reatha Diedrichs prepared the manuscript.

REFERENCES

Arritt, R. W., 1989: Numerical modeling of the offshore extent of sea breezes. *Quart. J. Roy. Meteor. Soc.,* **115,** 101–125.

——, 1993: Effects of the large-scale flow on characteristic features of the sea breeze. *J. Appl. Meteor.,* **32,** 116–125.

——, M. Segal, M. Leuthold, C. J. Anderson, and R. W. Turner, 1996: An observational study of the Lake Okeechobee lake breeze and its effect on deep convection. *Conf. on Coastal Oceanic and Atmospheric Prediction,* Atlanta, GA, Amer. Meteor. Soc., 350–353.

Curtim, E., D. W. Martin, and R. Rabin, 1995: Enhancement of cumulus clouds over deforested lands in Amazonia. *Bull. Amer. Meteor. Soc.,* **76,** 1801–1805.

Garratt, J. R., 1994: *The Atmospheric Boundary Layer*. Cambridge University, 316 pp.

Gibson, H. M., and T. H. Vonder Haar, 1990: Cloud and convection frequencies over the southeast United States as related to small-scale geographic features. *Mon. Wea. Rev.,* **118,** 2215–2227.

Gross, J. M., and M. A. Estoque, 1981: Further studies of a lake breeze. Part II: Theoretical Study. *Mon. Wea. Rev.,* **109,** 619–634.

Iribarne, J. V., and W. L. Godson, 1981: *Atmospheric Thermodynamics.* D. Reidel, 259 pp.

Nieuwstadt, F. T. M., and R. A. Brost, 1986: The decay of convective turbulence. *J. Atmos. Sci.,* **43,** 532–546.

Passareli, R. E., and R. R. Braham, 1981: The role of the winter land breeze in the formation of Great Lake snow storms. *Bull. Amer. Meteor. Soc.,* **62,** 482–491.

Physick, W., 1976: A numerical model of the sea-breeze phenomenon over a lake or gulf. *J. Atmos. Sci.,* **33,** 2107–2135.

Pielke, R. A., 1974: A three-dimensional numerical model of the sea breezes over south Florida. *Mon. Wea. Rev.,* **102,** 115–139.

Purdom, J. F. W., 1990: Convective scale weather analysis and forecasting. *Weather Satellites Systems, Data, and Environmental Application,* P. K. Rao, et al., Eds., Amer. Meteor. Soc., 285–304.

Rabin, R. N., P. J. Stadler, D. J. Stensrud, and M. Gregory, 1990: Observed effects of landscape variability on convective clouds. *Bull. Amer. Meteor. Soc.,* **71,** 272–280.

Segal, M., and R. A. Pielke, 1985: On the effect of water temperature and synoptic flows on the development of surface flows over narrow-elongated water bodies. *J. Geophys. Res.,* **90,** 4907–4910.

Siems, S. T., and C. B. Bretheron, 1992: A numerical investigation of cloud-top entrainment instability and related experiments. *Quart. J. Roy. Meteor. Soc.,* **118,** 787–818.